nature biotechnology

Metabolic engineering of *Escherichia coli* using synthetic small regulatory RNAs

Dokyun Na[1,2], Seung Min Yoo[1,2], Hannah Chung[1], Hyegwon Park[1], Jin Hwan Park[1,2] & Sang Yup Lee[1,2]

Small regulatory RNAs (sRNAs) regulate gene expression in bacteria. We designed synthetic sRNAs to identify and modulate the expression of target genes for metabolic engineering in *Escherichia coli*. Using synthetic sRNAs for the combinatorial knockdown of four candidate genes in 14 different strains, we isolated an engineered *E. coli* strain (*tyrR*- and *csrA*-repressed S17-1) capable of producing 2 g per liter of tyrosine. Using a library of 130 synthetic sRNAs, we also identified chromosomal gene targets that enabled substantial increases in cadaverine production. Repression of *murE* led to a 55% increase in cadaverine production compared to the reported engineered strain (XQ56 harboring the plasmid p15CadA)[1]. The design principles and the engineering strategy using synthetic sRNAs reported here are generalizable to other bacteria and applicable in developing superior producer strains. The ability to fine-tune target genes with designed sRNAs provides substantial advantages over gene-knockout strategies and other large-scale target identification strategies owing to its easy implementation, ability to modulate chromosomal gene expression without modifying those genes and because it does not require construction of strain libraries.

Metabolic engineering is an enabling technology for the isolation of microbial strains that can produce high yields of chemicals and materials from renewable resources. Identification of potential genetic targets and optimization of their expression are essential for efficient production of the desired metabolites. Several high-throughput strategies that modify chromosomal genes and DNA have been developed to improve product formation[2–5]. Nonetheless, the number of genes that can be manipulated is too low for such strategies to be applied at the genomic scale; for example, up to 24 genes can be successfully manipulated through multiplex automated genome engineering, but that figure represents <1% of the *E. coli* genome[3]. Another method, trackable recursive multiplex recombineering[5], uses a library of genomically barcoded strains to examine which gene(s) can increase production of a target product[6,7]. This strategy can be applied for genome-wide target identification, but it requires a pre-constructed library of different strains into which mutations and barcodes have already been introduced. There is a pressing need for a tool that enables genome-scale identification of suitable gene targets for engineering, identification of the best producer strain and fine-tuning of gene expression levels for the maximal production of desired chemicals without relying on pre-constructed libraries.

RNA-mediated regulatory mechanisms and their potential applications in synthetic biology[8–15] and metabolic engineering[16,17] have been well documented. The modularity, tunable base-pair complementation and *trans*-acting ability of RNA molecules can be exploited for genome-wide screening of effective target genes and for fine flux control (**Fig. 1a**). Owing to the absence of RNA interference in bacteria, there have been only a few studies of designed synthetic bacterial RNAs[9–12], and even fewer studies on the use of designed RNAs for metabolic engineering. Furthermore, most synthetic RNAs studied to date are synthetic riboswitches that are *cis*-acting and require a particular, context-dependent sequence alteration of the downstream secondary structure of mRNA, making them tricky to apply in metabolic engineering. The *trans*-acting sRNAs in bacteria were discovered about a decade ago[18]. However, owing to a lack of understanding about the RNA-silencing mechanisms in bacteria, only a few proof-of-concept studies designing synthetic sRNAs have been done, and these have relied on random screening[12,19,20] (**Supplementary Fig. 1**).

Here, we report the development of a general strategy for modulating gene expression at the translation stage using synthetic sRNAs that are rationally designed (rather than randomly screened)[18,21], and we provide proof-of-concept applications to metabolic engineering by increasing the production of tyrosine and cadaverine in *E. coli*. The synthetic sRNA–based strategy reported here is advantageous over conventional gene-knockout strategies and other large-scale target identification strategies because of its easy implementation and because it does not rely on pre-constructed strain libraries.

We developed synthetic sRNAs composed of two parts: a scaffold sequence and a target-binding sequence. Naturally occurring sRNAs in *E. coli* contain a consensus secondary structure that provides a scaffold for recruiting the Hfq protein, which facilitates the hybridization of sRNA and target mRNA as well as mRNA degradation. We screened the 101 *E. coli* sRNAs discovered to date for potential use as a scaffold[18,22] (**Supplementary Fig. 1**) and selected three candidates: SgrS, MicF and MicC[18,20]. To evaluate each candidate's potential for use in synthetic sRNAs, we replaced its target binding sequence with the antisense sequence to the translation initiation region (TIR) of DsRed2

[1]Metabolic and Biomolecular Engineering National Research Laboratory, Department of Chemical and Biomolecular Engineering (BK21 program), Korea Advanced Institute of Science and Technology (KAIST), Daejeon, Republic of Korea. [2]BioProcess Engineering Research Center, Bioinformatics Research Center, Center for Systems and Synthetic Biotechnology, Institute for the BioCentury, Korea Advanced Institute of Science and Technology (KAIST), Daejeon, Republic of Korea. Correspondence should be addressed to S.Y.L. (leesy@kaist.ac.kr).

Received 17 January 2012; accepted 22 November 2012; published online 20 January 2013; doi:10.1038/nbt.2461

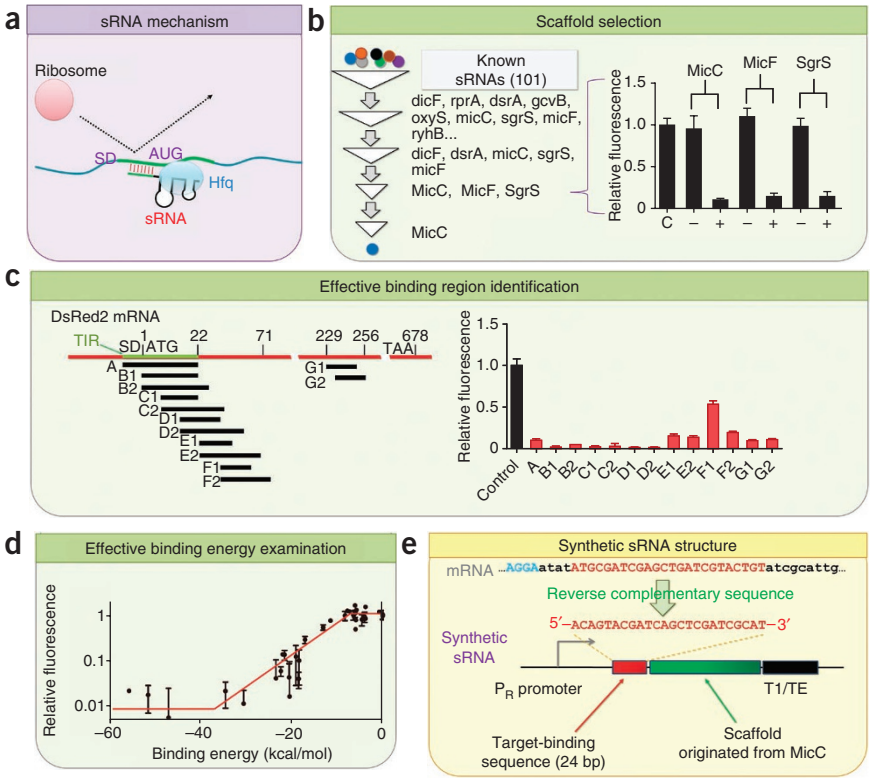

Figure 1 Design principles for synthetic sRNAs. (**a**) Mechanism of translation repression by sRNA. SD, Shine-Dalgarno sequence. (**b**) Scaffold selection process (**Supplementary Figs. 1** and **2**). C, no synthetic sRNA; –, scaffold without DsRed2-targeting sequence; +, scaffold with DsRed2-targeting sequence. Error bars, mean ± s.d. (**c**) The effect of binding region on repression efficiency. The letters denote binding sites of designed anti-DsRed2 synthetic sRNA variants (**Supplementary Fig. 3**). The location of TIR (green bar) was estimated using a previously published algorithm[24]. The intensity of DsRed2 that was not repressed by synthetic sRNAs was used as a control. All other intensities were normalized to the control. Error bars, mean ± s.d. (**d**) A quantitative relationship between synthetic sRNA binding energy and repression efficiency. Error bars, mean ± s.d. (**e**) The genetic structure of synthetic sRNA. T1/TE, transcriptional terminator (MITRegistry BBa_B0025). See **Supplementary Figure 6** for full sequence of synthetic sRNAs.

mRNA (**Supplementary Fig. 2**). We chose this TIR, which interacts with the ribosome[23] and spans from the Shine-Dalgarno sequence to the downstream 20–30 nucleotides, to interfere with ribosome binding to mRNA[21,23,24]. After examining synthetic sRNAs containing the SgrS, MicF and MicC scaffolds, we selected MicC as the final scaffold because of its superior repression capability (**Fig. 1b**).

In addition to the scaffold, another crucial part of a synthetic sRNA is the sequence that recognizes the target mRNA. First, we determined which mRNA regions are most responsive to sRNA-mediated repression. We designed anti-DsRed2 synthetic sRNAs with complementary sequences that bind completely or partially to the TIR of DsRed2 mRNA or to the regions outside of which the TIR was designed (**Fig. 1c** and **Supplementary Fig. 3**). The anti-DsRed2 sRNA variants targeting regions overlapping with the TIR (**Fig. 1c**) showed the highest repression (>90%), whereas others showed relatively inefficient repression[21,23,24]. We therefore chose the targeting region within the TIR for synthetic sRNA–based downregulation. We then investigated the quantitative relationship between binding energy and repression capability in order to achieve scalable repression with synthetic sRNAs. The target binding sequence of anti-DsRed2 sRNA was randomized through site-directed mutagenesis to generate diverse binding energies. The relative repression efficiencies of the synthetic sRNAs generated were estimated by measuring the changes in red fluorescence intensity. As shown in **Figure 1d**, the binding energy of anti-DsRed2 variants was correlated with repression capability, suggesting that binding energy–based forward engineering can generate diverse synthetic sRNAs with different repression capabilities and, furthermore, that those synthetic sRNAs can be used to fine-tune the expression of chromosomal genes. We confirmed the tunability of our synthetic sRNAs through modulation of *lacZ* expression by anti-*lacZ* sRNAs (**Supplementary Fig. 4**). In addition, introduction of up to three copies of sRNAs did not exert metabolic burden on the host cells (**Supplementary Fig. 5**).

On the basis of these results, we used MicC lacking the *ompC*-binding sequence as the scaffold for our synthetic sRNAs. OmpC forms an outer membrane porin for transporting hydrophilic solutes. To simplify the design process, we chose a binding sequence that is complementary to the coding sequence that spans the AUG to nucleotide +21 of the DsRed2 mRNA. This sequence is long enough to ensure high affinity but short enough to avoid cross-reaction (**Fig. 1e** and **Supplementary Figs. 6–8**). We also confirmed the possibility of employing synthetic sRNAs to regulate gene expression using a synthetic circuit (**Supplementary Fig. 9**).

To illustrate the potential use of synthetic sRNAs in metabolic engineering, we used them to identify both the *E. coli* strain having the highest metabolic capacity and the best repression target mRNAs in each strain. We also used synthetic sRNAs to fine-tune expression levels of repression targets to further increase production titers (**Supplementary Fig. 10**). We used this strategy to isolate an *E. coli* strain overproducing tyrosine, and we compared the results with those previously reported from a variety of metabolic engineering methods[25,26].

Even strains of the same *E. coli* species have different capacities for producing desired bioproducts[27]. But the hard-coded genetic reprogramming that underpins different metabolic capacities, even if isolated by traditional gene-knockout procedures, cannot be easily transferred to other strains without laborious iterative experiments. We evaluated the capacity for tyrosine production of 14 different *E. coli* strains: C600, DH5α, ER2925, JM110, MG1655, S17-1, T1R, TG1, TOP10, W3110 and XL1 (derived from *E. coli* strain K-12); BL21 (derived from *E. coli* strain B); W; and HB101 (a hybrid of the K-12 and B strains) (**Supplementary Table 1**).

We constructed an *E. coli* strain in which the genes *ppsA* (encoding phosphoenolpyruvate synthase), *tktA* (encoding transketolase A), *aroF* (encoding DAHP synthase), *aroK* (encoding shikimate kinase I) and *tyrC*[28] (encoding prephenate dehydrogenase originated from *Zymomonas mobilis*) and feedback-resistant *aroG* (encoding DAHP synthase with a D146N substitution) and *tyrA* (encoding chorismate mutase and prephenate dehydrogenase with M53I and A354V substitutions) mutants[25] were overexpressed to increase tyrosine pathway flux. We then selected four target genes for synthetic sRNA–based repression studies: *tyrR* (encoding tyrosine repressor), *csrA* (encoding

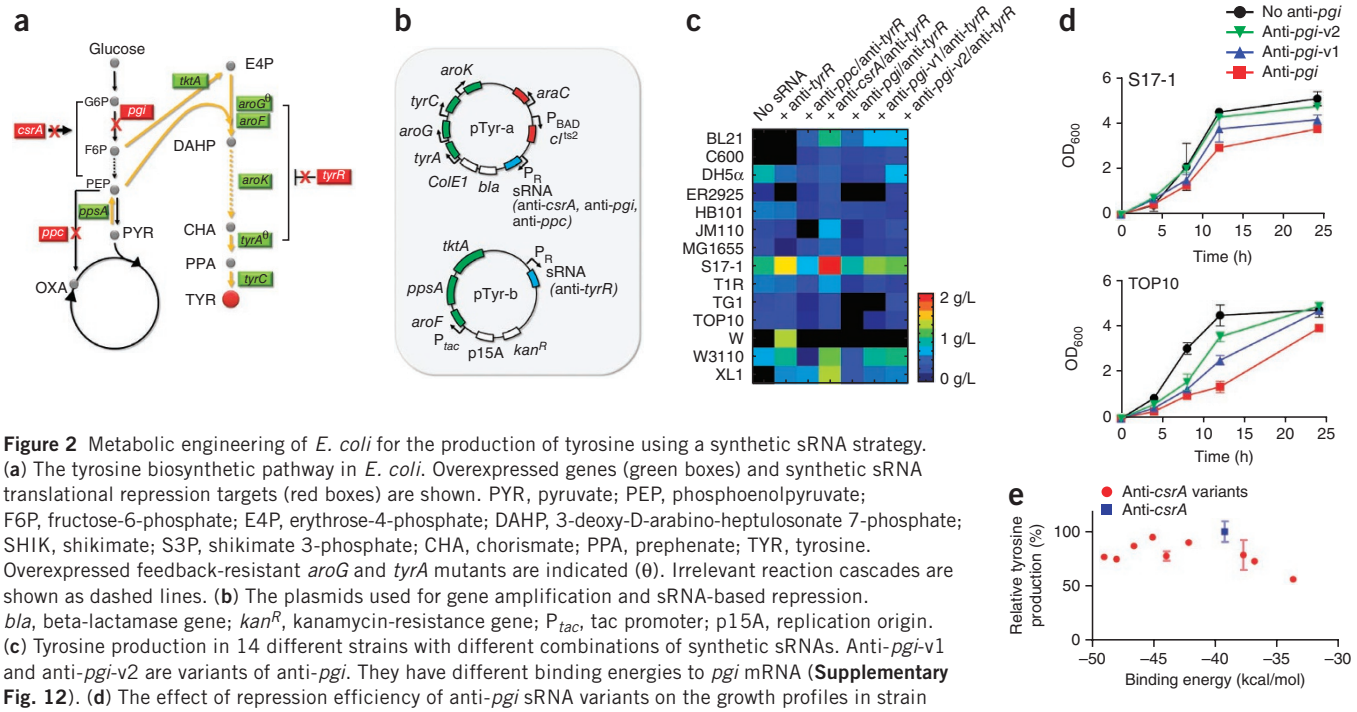

Figure 2 Metabolic engineering of *E. coli* for the production of tyrosine using a synthetic sRNA strategy. (**a**) The tyrosine biosynthetic pathway in *E. coli*. Overexpressed genes (green boxes) and synthetic sRNA translational repression targets (red boxes) are shown. PYR, pyruvate; PEP, phosphoenolpyruvate; F6P, fructose-6-phosphate; E4P, erythrose-4-phosphate; DAHP, 3-deoxy-D-arabino-heptulosonate 7-phosphate; SHIK, shikimate; S3P, shikimate 3-phosphate; CHA, chorismate; PPA, prephenate; TYR, tyrosine. Overexpressed feedback-resistant *aroG* and *tyrA* mutants are indicated (θ). Irrelevant reaction cascades are shown as dashed lines. (**b**) The plasmids used for gene amplification and sRNA-based repression. *bla*, beta-lactamase gene; kan^R, kanamycin-resistance gene; P_{tac}, tac promoter; p15A, replication origin. (**c**) Tyrosine production in 14 different strains with different combinations of synthetic sRNAs. Anti-*pgi*-v1 and anti-*pgi*-v2 are variants of anti-*pgi*. They have different binding energies to *pgi* mRNA (**Supplementary Fig. 12**). (**d**) The effect of repression efficiency of anti-*pgi* sRNA variants on the growth profiles in strain S17-1 (producing the highest concentration of tyrosine) or in TOP10 (producing the lowest concentration). See **Supplementary Figure 12** for detailed sequence information of anti-*pgi*-v1 and anti-*pgi*-v2. (**e**) Relative tyrosine production after fine-tuning of anti-*csrA* repression efficiency. Error bars, mean ± s.d. Tyrosine titers were normalized to the titer obtained from the engineered S17-1 strain which produced the highest concentration of tyrosine. Error bars, mean ± s.d.

carbon-storage regulator, which regulates the expression of enzyme genes involved in glycolysis), *pgi* (encoding phosphoglucose isomerase, which converts glucose-6-phosphate to fructose-6-phosphate) and *ppc* (encoding phosphoenolpyruvate carboxylase, which converts phosphoenolpyruvate to oxaloacetate) (**Fig. 2a**). To address the need for deregulation of the tyrosine biosynthetic pathway, we cloned anti-*tyrR* sRNA in combination with anti-*csrA*, anti-*pgi* or anti-*ppc* sRNA (**Fig. 2b**). We evaluated synthetic sRNA combinations in all strains and observed strain-to-strain variations in tyrosine titer (**Fig. 2c**) that were due to differences not in synthetic sRNA efficiency but in metabolic capability among strains (**Supplementary Fig. 11**). Among the sRNA combinations, anti-*tyrR* and anti-*csrA* in S17-1 produced the highest tyrosine titer (2.0 g per liter) compared with other strains, which produced 0–1.3 g tyrosine per liter (**Fig. 2c**). This tyrosine titer is on par with that obtained from the most productive strain reported recently, in which proteomic and metabolomic analyses were used to guide the modification of promoters, plasmid copy numbers and operon arrangement to optimize the expression levels of various genes[26].

The decrease in tyrosine titer upon the introduction of anti-*pgi* sRNA into strains harboring anti-*tyrR* was probably due to the decreased rate of cell growth[29,30] (**Fig. 2d**). To examine whether fine-tuning of *pgi* expression level can balance the metabolic flux between cell growth and product formation, we generated two anti-*pgi* sRNA variants by forward engineering (**Supplementary Fig. 12**). In all strains, the anti-*pgi* sRNA variants increased tyrosine production and growth rate compared with the original anti-*pgi* sRNA (**Fig. 2c,d**), indicating that synthetic sRNAs can finely modulate metabolic flux to achieve a balance between biomass and the desired product.

We did not observe increases in tyrosine titers after additional co-repression of anti-*ppc* or the anti-*pgi* variants or introduction of the newly constructed library of 84 synthetic sRNAs into the engineered S17-1 strain harboring anti-*tyrR* and anti-*csrA* (**Supplementary Figs. 13** and **14**), which indicates that repression of *tyrR* and *csrA* is the most effective strategy for increasing tyrosine production in S17-1 cells. We verified the results of our synthetic sRNA experiments by gene knockout in strain S17-1 (**Supplementary Fig. 15**).

To examine whether fine-tuning of the anti-*csrA* sRNA can be used to modulate cellular fluxes, we generated anti-*csrA* sRNA variants by forward engineering and introduced them into strain S17-1 harboring anti-*tyrR*. We identified the optimal level of *csrA* repression for maximizing tyrosine production (**Fig. 2e**). Among sRNAs tested, use of the synthetic sRNA with a binding energy of –39.2 kcal mol^{-1} resulted in the highest tyrosine titer. Finally, high-cell-density cultivation of the best strain enabled tyrosine production of up to 21.9 g per liter (**Supplementary Fig. 16**).

We also used a synthetic sRNA–based strategy to increase the production of cadaverine, an important nylon precursor. We used the previously engineered *E. coli* strain XQ56 harboring plasmid p15CadA, (producing lysine decarboxylase, which converts lysine to cadaverine) which can produce 1.4 g cadaverine per liter, as the starting strain[1]. We chose eight genes encoding enzymes responsible for diverting the metabolic fluxes from cadaverine formation as candidate targets for modulation by synthetic sRNAs (**Supplementary Fig. 17**). Of the six synthetic sRNAs found to increase cadaverine titers, the best-performing one was anti-*murE*, which reduced the outflux for cell wall synthesis and increased the cadaverine titer to 2.15 g per liter.

To facilitate large-scale target identification with synthetic sRNAs, we constructed a library of 122 synthetic sRNAs that repress the expression of genes involved in cadaverine production or regulatory pathways (**Fig. 3a**). We introduced plasmids harboring each of the 122 synthetic sRNAs individually into starting strain XQ56 harboring p15CadA (**Fig. 3b**). Among the 31 synthetic sRNAs that increased cadaverine production (**Supplementary Tables 2** and **3**), the sRNAs

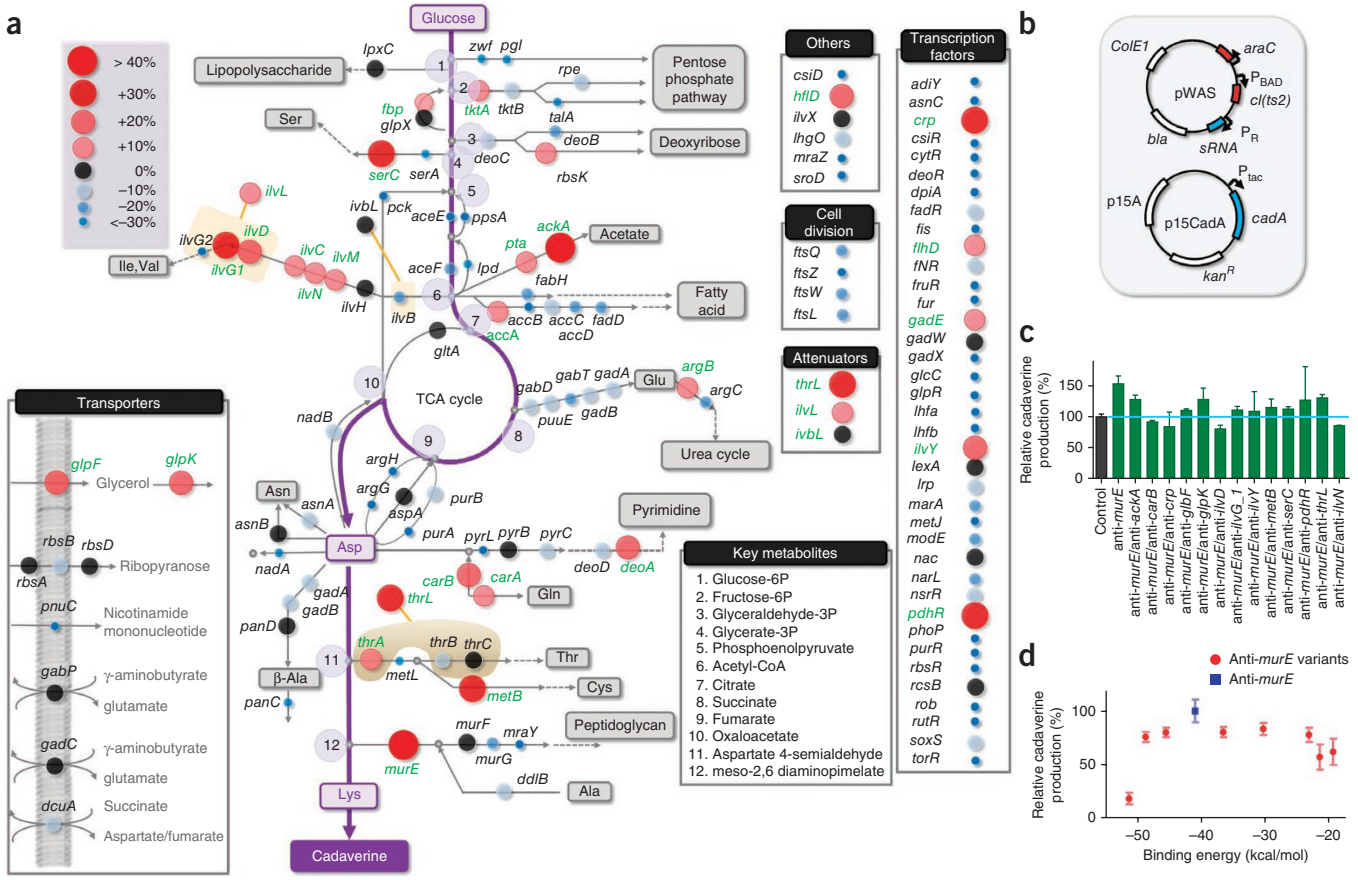

Figure 3 Synthetic sRNA–based strategy for large-scale target identification and fine-tuning of gene expression for enhanced cadaverine production. (**a**) Schematic of the cadaverine biosynthetic pathway in *E. coli*, from glycolysis through lysine biosynthesis and single-step conversion to cadaverine by lysine decarboxylase[1]. The 130 target genes are shown (see **Supplementary Table 2**). Relative changes in cadaverine titer compared with the base strain are represented as colored circles. Black circle represents no significant (0%) increase in cadaverine production compared to the previously constructed base strain (1.4 g per liter)[1]. Synthetic sRNA targets that increased cadaverine titer are shown in green (relationships among transcription factors and genes are listed in **Supplementary Table 3**). (**b**) Plasmid constructs for the expression of the *cadA* gene and for regulated production of synthetic sRNAs. (**c**) Effects of combinatorial introduction of synthetic sRNAs on cadaverine production. The cadaverine titer obtained from the base strain was set to 100% (control). (**d**) Relative cadaverine production obtained using anti-*murE* variants. The titer obtained using anti-*murE* was set to 100%. Error bars in **c** and **d**, mean ± s.d.

targeting *ackA* (encoding propionate kinase 2) and *pdhR* (encoding pyruvate dehydrogenase complex regulator), both of which are not present in the main cadaverine biosynthetic pathways, increased cadaverine titers by 40.2% and 31.4%, respectively. These results may indicate that a synthetic sRNA–based strategy can be used for the identification of effective and, in particular, non-obvious target genes that could be manipulated for the enhanced production of a desired bioproduct.

The top-ranked target genes were *murE* and *ackA*, which were identified by rational selection and system-wide approaches, respectively, as described above. It should be noted that *murE* and *ackA* are essential genes; therefore, they cannot be identified by gene-knockout experiments, conferring an additional advantage of a synthetic sRNA–based strategy over a conventional gene-knockout strategy. Combinatorial repression by anti-*murE*, which enabled the highest cadaverine titers, and sRNAs repressing the other top 13 target genes did not further increase cadaverine titer (**Fig. 3c**).

We engineered anti-*murE* variants to fine-tune the expression level of *murE* (**Fig. 3d**) and confirmed synthetic sRNA-mediated tuning of MurE protein expression by two-dimensional (2D)-PAGE analyses (**Supplementary Fig. 18**). As with *csrA*, an optimal repression level of *murE* enabled maximal cadaverine production. Among the variants constructed, the sRNA having a binding energy of –40.9 kcal mol^{-1} allowed the highest cadaverine titer. High-cell-density cultivation of the engineered strain expressing the most effective anti-*murE* sRNA variant led to the production of 12.6 g cadaverine per liter, which is 31% higher than that obtained with starting strain XQ56 harboring p15CadA (9.6 g per liter) (**Supplementary Fig. 19**).

The results obtained for both tyrosine and cadaverine production indicate that our synthetic sRNA–based strategy can be used both for metabolic engineering of bacterial strains (including initial strain selection) and for improvement of already-engineered strains through large-scale identification of effective target genes and fine-tuning of their expression levels.

One benefit of synthetic sRNAs is their ability to modulate chromosomal gene expression without the modification of chromosomal sequences. Once a superior platform strain and effective target genes have been identified through synthetic sRNA screening, various strategies for systems metabolic engineering can be used for further strain improvement. In addition, the expression levels of genes cloned into plasmids for overexpression studies could be optimized using a combinatorial ribosome–binding site optimization strategy[2] or

promoter-strength optimization[4]. In summary, the synthetic sRNA–based strategy presented here enables the rapid development of high-performance microbial strains.

METHODS

Methods and any associated references are available in the online version of the paper.

Note: Supplementary information is available in the online version of the paper.

ACKNOWLEDGMENTS

We would like to thank M.-H. Lee for measuring tyrosine and cadaverine concentrations using high-performance liquid chromatography, Y.H. Lee for 2D-PAGE experiments, J.A. Im for large-scale cloning of synthetic sRNAs and cultivation experiments, and S.J. Choi for fermentation experiments. This work was supported by the Technology Development Program to Solve Climate Changes on Systems Metabolic Engineering for Biorefineries (NRF-2012-C1AAA001-2012M1A2A2026556); the Intelligent Synthetic Biology Center through the Global Frontier Project (2011-0031963) of the Ministry of Education, Science and Technology (MEST) through the National Research Foundation of Korea; and the World Class University program (R32-2008-000-10142-0) of MEST.

AUTHOR CONTRIBUTIONS

S.Y.L. and D.N. conceived of the project. D.N. designed the structure of synthetic sRNAs and performed sRNA construction and evaluation and metabolic engineering experiments. S.M.Y. performed sRNA construction and evaluation and metabolic engineering experiments. H.C. and H.P. carried out large-scale screening for cadaverine production. J.H.P. constructed the S17-1 knockout strain and performed fermentation experiments. S.Y.L. supervised the project. All authors contributed to the preparation of the manuscript.

COMPETING FINANCIAL INTERESTS

The authors declare no competing financial interests.

Published online at http://www.nature.com/doifinder/10.1038/nbt.2461.
Reprints and permissions information is available online at http://npg.nature.com/reprintsandpermissions/.

1. Qian, Z.-G., Xia, X.-X. & Lee, S.Y. Metabolic engineering of *Escherichia coli* for the production of cadaverine: a five-carbon diamine. *Biotechnol. Bioeng.* **108**, 93–103 (2011).
2. Pfleger, B.F., Pitera, D.J., Smolke, C.D. & Keasling, J.D. Combinatorial engineering of intergenic regions in operons tunes expression of multiple genes. *Nat. Biotechnol.* **24**, 1027–1032 (2006).
3. Wang, H.H. *et al.* Programming cells by multiplex genome engineering and accelerated evolution. *Nature* **460**, 894–898 (2009).
4. Sharon, E. *et al.* Inferring gene regulatory logic from high-throughput measurements of thousands of systematically designed promoters. *Nat. Biotechnol.* **30**, 521–530 (2012).
5. Sandoval, N.R. *et al.* Strategy for directing combinatorial genome engineering in *Escherichia coli*. *Proc. Natl. Acad. Sci. USA* **109**, 10540–10545 (2012).
6. Ho, C.H. *et al.* A molecular barcoded yeast ORF library enables mode-of-action analysis of bioactive compounds. *Nat. Biotechnol.* **27**, 369–377 (2009).
7. Kress, W.J. & Erickson, D.L. DNA barcodes: genes, genomics, and bioinformatics. *Proc. Natl. Acad. Sci. USA* **105**, 2761–2762 (2008).
8. Saito, H. & Inoue, T. Synthetic biology with RNA motifs. *Int. J. Biochem. Cell Biol.* **41**, 398–404 (2009).
9. Desai, S.K. & Gallivan, J.P. Genetic screens and selections for small molecules based on a synthetic riboswitch that activates protein translation. *J. Am. Chem. Soc.* **126**, 13247–13254 (2004).
10. Isaacs, F.J. *et al.* Engineered riboregulators enable post-transcriptional control of gene expression. *Nat. Biotechnol.* **22**, 841–847 (2004).
11. Carothers, J.M., Goler, J.A., Juminaga, D. & Keasling, J.D. Model-driven engineering of RNA devices to quantitatively program gene expression. *Science* **334**, 1716–1719 (2011).
12. Sharma, V., Yamamura, A. & Yokobayashi, Y. Engineering artificial small RNAs for conditional gene silencing in *Escherichia coli*. *ACS Synth. Biol.* **1**, 6–13 (2012).
13. Liang, J.C., Bloom, R.J. & Smolke, C.D. Engineering biological systems with synthetic RNA molecules. *Mol. Cell* **43**, 915–926 (2011).
14. Win, M.N. & Smolke, C.D. Higher-order cellular information processing with synthetic RNA devices. *Science* **322**, 456–460 (2008).
15. Lucks, J.B., Qi, L., Mutalik, V.K., Wang, D. & Arkin, A.P. Versatile RNA-sensing transcriptional regulators for engineering genetic networks. *Proc. Natl. Acad. Sci. USA* **108**, 8617–8622 (2011).
16. Delebecque, C.J., Lindner, A.B., Silver, P.A. & Aldaye, F.A. Organization of intracellular reactions with rationally designed RNA assemblies. *Science* **333**, 470–474 (2011).
17. Kang, Z., Wang, X., Li, Y., Wang, Q. & Qi, Q. Small RNA RyhB as a potential tool used for metabolic engineering in *Escherichia coli*. *Biotechnol. Lett.* **34**, 527–531 (2012).
18. Gottesman, S. The small RNA regulators of *Escherichia coli*: Roles and mechanisms. *Annu. Rev. Microbiol.* **58**, 303–328 (2004).
19. Man, S. *et al.* Artificial trans-encoded small non-coding RNAs specifically silence the selected gene expression in bacteria. *Nucleic Acids Res.* **39**, e50 (2011).
20. Urban, J.H. & Vogel, J. Translational control and target recognition by *Escherichia coli* small RNAs *in vivo*. *Nucleic Acids Res.* **35**, 1018–1037 (2007).
21. Aiba, H. Mechanism of RNA silencing by Hfq-binding small RNAs. *Curr. Opin. Microbiol.* **10**, 134–139 (2007).
22. Pichon, C., du Merle, L., Caliot, M.E., Trieu-Cuot, P. & Le Bouguénec, C. An *in silico* model for identification of small RNAs in whole bacterial genomes: characterization of antisense RNAs in pathogenic *Escherichia coli* and *Streptococcus agalactiae* strains. *Nucleic Acids Res.* **40**, 2846–2861 (2012).
23. Culver, G.M. Meanderings of the mRNA through the ribosome. *Structure* **9**, 751–758 (2001).
24. Na, D., Lee, S. & Lee, D. Mathematical modeling of translation initiation for the estimation of its efficiency to computationally design mRNA sequences with a desired expression level in prokaryotes. *BMC Syst. Biol.* **4**, 71 (2010).
25. Lütke-Eversloh, T. & Stephanopoulos, G. L-tyrosine production by deregulated strains of *Escherichia coli*. *Appl. Microbiol. Biotechnol.* **75**, 103–110 (2007).
26. Juminaga, D. *et al.* Modular engineering of L-tyrosine production in *Escherichia coli*. *Appl. Environ. Microbiol.* **78**, 89–98 (2012).
27. Lee, S.Y., Lee, K.M., Chan, H.N. & Steinbüchel, A. Comparison of recombinant *Escherichia coli* strains for synthesis and accumulation of poly-(3-hydroxybutyric acid) and morphological changes. *Biotechnol. Bioeng.* **44**, 1337–1347 (1994).
28. Lütke-Eversloh, T. & Stephanopoulos, G. Combinatorial pathway analysis for improved L-tyrosine production in *Escherichia coli*: identification of enzymatic bottlenecks by systematic gene overexpression. *Metab. Eng.* **10**, 69–77 (2008).
29. Hua, Q., Yang, C., Baba, T., Mori, H. & Shimizu, K. Responses of the central metabolism in *Escherichia coli* to phosphoglucose isomerase and glucose-6-phosphate dehydrogenase knockouts. *J. Bacteriol.* **185**, 7053–7067 (2003).
30. Kadir, T.A., Mannan, A., Kierzek, A., McFadden, J. & Shimizu, K. Modeling and simulation of the main metabolism in *Escherichia coli* and its several single-gene knockout mutants with experimental verification. *Microb. Cell Fact.* **9**, 88 (2010).

ONLINE METHODS

Strains, media and culture conditions. *E. coli* DH5α cells used as a host strain for DNA manipulation were cultured routinely, in LB medium (10 g Bacto Tryptone, 5 g yeast extract and 10 g NaCl per liter) with appropriate antibiotics at 37 °C. DH5α was also used as a host strain and cultured in LB medium for the experiments of sRNA scaffold efficiency evaluation (**Fig. 1b**), effective binding region identification in mRNA (**Fig. 1c**) and fine-tuning of sRNA efficiency (**Fig. 1d**).

For tyrosine production experiments, 14 different *E. coli* strains were used: BL21(DE3) (referred to as BL21), C600, DH5α, ER2925, HB101, JM110, MG1655, S17-1, T1R (ccdB survival T1 phage resistant cell; Invitrogen), TG1, TOP10 (Invitrogen), W, W3110, and XL1-Blue (referred to as XL1) (genotypes are listed in **Supplementary Table 1**). Engineered *E. coli* strains were cultured in LB medium with appropriate antibiotics and 1% arabinose at 25 °C until they reached stationary phase. Cells were then transferred to a baffled flask containing 50 ml of fresh medium without arabinose (6.75 g KH_2PO_4, 2 g $(NH_4)_2HPO_4$, 0.85 g citric acid, 3 g yeast extract, 20 g glucose and 10 ml trace metal solution per liter; pH 6.8) and cultured at 37 °C to initiate the production of synthetic sRNA (see below for details of regulating synthetic sRNA production). The composition of the trace metal solution is 10 g $FeSO_4•7H_2O$, 2.2 g $ZnSO_4•7H_2O$, 0.58 g $MnSO_4•4H_2O$, 1 g $CuSO_4•5H_2O$, 0.1 g $(NH_4)_6Mo_7O_{24}•4H_2O$, 0.2 g $Na_2B_4O_7•10H_2O$ and 10 ml of 35% HCl per liter. Cells were harvested and tyrosine titers were measured 48 h after inoculation.

For cadaverine production, *E. coli* strain XQ56 harboring p15CadA plasmid was used as a base strain[1]. XQ56 harboring p15CadA plasmid and pWAS plasmid harboring synthetic sRNA (**Fig. 3b**) was cultured in LB medium with appropriate antibiotics and 1% arabinose at 25 °C until reaching stationary phase. Then, cells were transferred to a baffled flask containing 50 ml of fresh medium without arabinose (6.75 g KH_2PO_4, 2 g $(NH_4)_2HPO_4$, 3 g $(NH_4)_2SO_4$, 0.85 g citric acid, 0.7 g $MgSO_4•7H_2O$, 20 g glucose and 5 ml trace metal solution per liter; pH 6.8) and incubated at 37 °C as previously reported[1]. Cells were harvested and cadaverine titers were measured 24 h after inoculation.

DNA manipulation and plasmid construction. The oligonucleotide primers and PCR templates used for constructing synthetic sRNAs, cloning genes used in this study and knocking out *tyrR* and *csrA* genes are listed in **Supplementary Sequences**.

For the efficiency evaluation of MicC, SgrS and MicF as scaffolds, each was cloned into a plasmid harboring the ColE1 replication origin and the gene encoding DsRed2 under the control of a *Lac* promoter. The three sRNAs were designed to be produced by phage λ P_R promoter (MITRegistry, BBa_R0051) and transcriptionally terminated by T1/TE (MITRegistry, BBa_B0025) (**Supplementary Fig. 2**). Then, the inherent target-binding sequences of the scaffolds were replaced with a complementary sequence to the DsRed2 TIR through site-directed mutagenesis, and the intensity changes of DsRed2 fluorescence were measured to assess the efficiencies of the scaffolds.

A plasmid construct harboring the genes encoding DsRed2 and the MicC scaffold was used to identify the effective synthetic sRNA targeting regions in mRNA. Target-binding sequences complementary to various regions of DsRed2 mRNA were inserted between the scaffold sequence and its promoter sequence through site-directed mutagenesis. The target binding sequences are shown in **Supplementary Figure 3**. When compared to the intensity of DsRed2 that was not repressed by any synthetic sRNAs, changes in the intensity of DsRed2 fluorescence after insertion of the various synthetic sRNAs were measured.

For the experiments investigating the quantitative relationship between binding energy of synthetic sRNA and repression efficiency, the target-binding sequence of anti-DsRed2 synthetic sRNA constructed for identifying effective targeting regions was replaced with random nucleotides to generate diverse binding energies through site-directed mutagenesis (**Supplementary Sequences**). Repression efficiencies were measured by assaying DsRed2 fluorescence intensity with and without synthetic sRNA. Binding energies were calculated using UNAfold software[31].

Several genes for enhancing the tyrosine biosynthetic pathway and driving greater metabolic flux from central metabolic pathways to tyrosine biosynthesis were cloned as part of metabolic engineering efforts to produce tyrosine. *ppsA* (encoding phosphoenolpyruvate synthase), *tktA* (encoding transketolase I), *aroF* (encoding DAHP synthase), *aroG* (encoding DAHP synthase), *aroK* (encoding shikimate kinase I) and *tyrA* (encoding chorismate mutase/prephenate dehydrogenase) genes were cloned from *E. coli* W3110. The gene encoding TyrC (prephenate dehydrogenase), which converts prephenate directly to tyrosine, was cloned from *Zymomonas mobilis*. We constructed a feedback-resistant *aroG* (encoding a D146N substitution) and *tyrA* (encoding M53I and A354V substitutions) genes by site-directed mutagenesis[25]. For the tight regulation of synthetic sRNA production, we also incorporated a dual regulation system composed of *araC* and P_{BAD}-cI^{ts2} (**Fig. 2b**). The cI^{ts2} protein has a temperature-sensitive substitution mutation (K224E).

As synthetic sRNAs targeting essential genes would disrupt or retard cell growth, a tight regulation system was developed to switch their production off during the pre-culture phase and on during the production phase (**Figs. 2b** and **3b**). The regulation system consists of a constitutively expressed AraC protein gene, a temperature-sensitive cI^{ts2} gene[32] under the control of the P_{BAD} promoter and a gene encoding synthetic sRNA under the control of phage λ P_R promoter. At permissive temperature (25 °C) and with 1% arabinose, AraC protein is activated by arabinose and then activates the P_{BAD} promoter to produce cI^{ts2} protein. At 25 °C, cI^{ts2} maintains its activity to repress transcription from the P_R promoter and thereby blocks the production of synthetic sRNA. At nonpermissive temperature (37 °C) and in the absence of arabinose, AraC protein fails to activate the production of cI^{ts2} protein. Thus, the P_R promoter is switched on owing to the absence of cI^{ts2} and, consequently, the downstream synthetic sRNA-encoding gene is expressed. Even in the case of leaky production of cI^{ts2} protein, the temperature-sensitive mutation makes the protein nonfunctional at 37 °C. Therefore, cells were manipulated and incubated at 25 °C with 1% arabinose during the pre-culture phase and were transferred to medium without arabinose and incubated at 37 °C during the production phase. This dual regulation system tightly regulates synthetic sRNA production and allows conditional chromosomal gene repression as designed.

For improving cadaverine production, a library of synthetic sRNAs targeting 130 different chromosomal genes was constructed. The 130 target genes comprise those encoding enzymes that consume the flux from glycolysis (37 genes); those involved in the TCA cycle (8 genes), the lysine biosynthetic pathway (29 genes) or other major metabolic pathways (18 genes); and 38 genes encoding transcription factors that regulate the transcription of many of these genes (genes are listed in **Supplementary Tables 2** and **3**). The synthetic sRNAs were constructed through site-directed mutagenesis using the pWAS plasmid as a template and the oligonucleotides listed in **Supplementary Sequences**. Constructed plasmids harboring synthetic sRNAs were transformed into the cadaverine production strain (XQ56 carrying p15CadA)[1]. For tight regulation of synthetic sRNA production, the dual regulation system used for tyrosine production was also additionally cloned into the plasmid (**Fig. 3b**).

For fine-tuning of anti-*csrA* and anti-*murE* synthetic sRNAs, the sRNA target-binding sequences were randomized to generate diverse binding energies through site-directed mutagenesis using the oligonucleotides listed in **Supplementary Sequences**. Anti-*csrA* variants were cloned into pTyr-a plasmid for tyrosine production. The plasmids harboring an anti-*murE* variant were transformed into the XQ56 strain harboring p15CadA plasmid for cadaverine production.

Evaluation of synthetic sRNA efficiencies. Cells transformed with a plasmid producing sRNA and the reporter protein (DsRed2) were grown until they reached stationary phase. DsRed2 fluorescence was measured using a FACSCalibur Flow Cytometry System (Becton Dickinson). Measured intensities were adjusted by subtracting the autofluorescence intensity emitted from cells without DsRed2 gene. The adjusted fluorescence intensities were then normalized to the red fluorescence intensity measured from the cells harboring the gene encoding DsRed2 without the synthetic sRNA gene or with the synthetic sRNA gene containing the scaffold sequence only.

Tyrosine or cadaverine assay. Samples were centrifuged at 5,000 r.p.m. for 10 min to separate medium from cells, and supernatant was used for assay. For the tyrosine assay, pH of samples was adjusted to 1 by adding 1/10 volume of HCl, and tyrosine in dissolved medium was detected by measuring

absorbance at 210 nm using a high-performance liquid chromatography (HPLC) system equipped with a Zorbax SB-Aq column (3 × 250 mm; Agilent Technologies) using 20 mM 1-hexanesulfonic acid (pH 2.0, adjusted using H_3PO_4) as a stationary phase and acetonitrile as a mobile phase. For cadaverine assay, cadaverine concentration was determined by pre-column *O*-phthaldialdehyde derivatization coupled with HPLC and UV detection as previously reported[1].

Cell growth-rate assay. DH5α cells harboring between zero and four synthetic sRNAs were grown in LB medium, and 1/100 of the total volume was added to a 100-well plate containing LB medium. The plate was incubated with shaking at 37 °C in BioScreenC (Oy Growth Curves Ab Ltd, Finland). We recorded the optical density of the cells harboring different numbers of synthetic sRNAs in the exponential phase. The growth profile was then fitted to the exponential growth equation $y = y_0 e^{(kt)}$, where y_0 is the initial OD_{600}; k is the growth rate constant and t is time. The equation is an integral form of $dy/dt = k \times y$.

Two-dimensional gel electrophoresis analysis. 2D-PAGE experiments were performed as described previously[33]. Cells were suspended and mixed with a lysis buffer (8 M urea, 2 M thiourea, 40 mM Tris, 65mM DTT and 4% (wt/vol) CHAPS). Proteins in supernatant (200 μg) were diluted into 340 μl of rehydration buffer (8 M urea, 2 M thiourea, 20 mM DTT, 2% (wt/vol) CHAPS, 0.8% (wt/vol) immobilized pH gradient (IPG) buffer and 1% (vol/vol) cocktail protease inhibitor) and then loaded onto Immobiline DryStrip gels (18 cm, pH 3–10 NL; GE Healthcare). The loaded IPG strips were rehydrated, focused and equilibrated. The equilibrated strips were transferred to 12% (wt/vol) SDS-polyacrylamide gels. The 2D image was analyzed using PDQuest 2D Analysis Software (Bio-Rad). The protein spots in the 2D gel were identified by comparison with a previous report[34] and the *E. coli* 2D database (http://world-2dpage.expasy.org/swiss-2dpage/viewer).

31. Markham, N.R. & Zuker, M. UNAFold: software for nucleic acid folding and hybridization. *Methods Mol. Biol.* **453**, 3–31 (2008).
32. Jana, N.K., Roy, S., Bhattacharyya, B. & Mandal, N.C. Amino acid changes in the repressor of bacteriophage λ due to temperature-sensitive mutations in its cI gene and the structure of a highly temperature-sensitive mutant repressor. *Protein Eng.* **12**, 225–233 (1999).
33. Xia, X.-X. Native-sized recombinant spider silk protein produced in metabolically engineered *Escherichia coli* results in a strong fiber. *Proc. Natl. Acad. Sci. USA* **107**, 14059–14063 (2010).
34. Pasquali, C. *et al.* Two-dimensional gel electrophoresis of *Escherichia coli* homogenates: the *Escherichia coli* SWISS-2DPAGE database. *Electrophoresis* **17**, 547–555 (1996).

doi:10.1038/nbt.2461